NANO LETTERS

2007
Vol. 7, No. 5
1224−1231

Counterintuitive Effect of Molecular Strength and Role of Molecular Rigidity on Mechanical Properties of Layer-by-Layer Assembled Nanocomposites

Paul Podsiadlo,[†] Zhiyong Tang,[||] Bong Sup Shim,[†] and Nicholas A. Kotov*[,†,‡,§]

Departments of Chemical Engineering, Materials Science and Engineering, and Biomedical Engineering, University of Michigan, Ann Arbor, Michigan 48109, and Center for Nanoscience and Nanotechnology, Beijing, China

Received January 10, 2007; Revised Manuscript Received February 22, 2007

ABSTRACT

Molecular engineering of multilayered composites by layer-by-layer assembly (LBL) made possible easy replication of mechanical properties of nacre. Taking advantage of the ability of LBL to finely control the structure of the composite, one can further improve the mechanical properties of the multilayers, e.g., increase the strength and stiffness, and gain better understanding of the nanoscale and molecular scale mechanics of the materials critical for a variety of advanced technologies. In this study, we have replaced poly(diallyldimethylammonium chloride) (PDDA) (σ_{UTS} ∼12 MPa, E ∼0.2 GPa) with a much stronger polysaccharide polycation, chitosan (CH, σ_{UTS} ∼108 MPa, E ∼2 GPa), considering that its superior molecular strength will improve the macroscale mechanical properties of the nanocomposite: strength and stiffness. Free-standing films of the CH and montmorillonite (MTM) have been successfully made, and the resulting films revealed high uniformity with very high loading of MTM closely comparable to that in the natural nacre, ∼80 wt %. Contrary to our expectations and theoretical predictions, the CH–MTM composite revealed lower strength and stiffness than those of PDDA–MTM and lower strength than CH polymer itself: $\sigma_{UTS} \approx 80$ MPa and $E \approx 6$ GPa. Analysis of the morphology of adsorbing CH chains with atomic force microscopy revealed highly elongated molecules, which is opposite to the observations made for PDDA. Plane-to-plane adhesion showed a factor of ∼4 lower strength when compared to PDDA–MTM nanocomposite. Altogether these facts support the conclusion that CH lacks flexibility necessary for strong adhesion and efficient load transfer between the organic matrix and MTM platelets. High rigidity of the CH chains does not allow them to acquire a conformation necessary for maximizing the interfacial attraction with nanoscale component of the composite. These observations create an important foundation in the experimental design of the high-performance nanocomposite materials.

The layer-by-layer (LBL) assembly technique, based on sequential adsorption of oppositely charged compounds, is one of the most popular and well-established methods for preparation of multilayered thin films. LBL was first demonstrated for oppositely charged polyelectrolytes (PEs) in the early 1990s by Decher et al.,[1] and since then there has been virtually an explosion in the amount of scientific literature in this field. The technique has gained its popularity due to its ability to form highly tuned, functional films with nanometer-level control as well as due to its simplicity, requiring a minimum of setup and inexpensive equipment.[2]

The LBL technique is applicable for more than only pure PE systems. Almost any type of charged species including inorganic molecular clusters,[3] nanoparticles,[4] nanotubes and nanowires,[5,6] nanoplates,[7] organic dyes,[8] dendrimer,[9] porphyrin,[10] polysaccharides,[11,12] polypeptides,[13] nucleic acids and DNA,[14] proteins,[15,16] and viruses[17] can be successfully used as the components to prepare thin films.[18] The technique has led to a number of novel designs and applications, e.g., superhydrophobic surfaces,[19,20] chemical sensors and semipermeable membranes,[18,21−23] drug and biomolecules delivery systems,[18,24,25] optically active and responsive films,[26−28] cell and protein adhesion resistant coatings,[18,29] fuel cells and photovoltaic materials,[30] biomimetic and bioresponsive coatings,[20,31] semiconductors,[32,33] catalysts,[34,35] and magnetic devices[36,37] to name a few.[2,18]

LBL assembly has proven invaluable in its ability to merge the functionalities of multiple components. Through creative

* To whom correspondence should be addressed: tel, (734) 763-8768; fax, (734) 764-7453; e-mail, kotov@umich.edu.
[†] Department of Chemical Engineering, University of Michigan.
[‡] Department of Materials Science and Engineering, University of Michigan.
[§] Department of Biomedical Engineering, University of Michigan.
[||] Center for Nanoscience and Nanotechnology.

10.1021/nl0700649 CCC: $37.00
Published on Web 04/25/2007

experimental setup, one can, for example, combine the physical properties of nanoparticles (NPs) and proteins with the mechanical properties of clays and polymers. Our group has found that LBL assembly of a polyelectrolyte poly(diallyldimethylammonium chloride) (PDDA) and Na^+-montmorillonite (MTM) can lead to a free-standing film with mechanical properties similar to those of seashell nacre and lamellar bones.[38] In fact, the mechanical properties of this material (ultimate strength, $\sigma_{UTS} = 100 \pm 10$ MPa and the Young's modulus, $E = 11 \pm 2$ GPa), exceed those of many clay composites prepared by simple dispersion. At the molecular level, the assembly of MTM has found several applications. The monolayers of MTM have been used to control interactions between layers of gold NPs[39] and combined assemblies of MTM and magnetite NPs have led to free-standing magnetic films.[37] Recently, we have also shown the ability of the LBL technique to impart additional functionalities into this material. Taking advantage of its mechanical properties, we have incorporated biocompatible silver NPs and thus have generated a strong thin film coating with excellent antibacterial properties, biocompatibility, and long term stability.[40] Other examples of LBL assemblies incorporating MTM nanosheets include preparation of LBL films of myoglobin or horseradish peroxide for voltammetry studies, photocontrollable magnetic thin films, chemiluminescent thin films for sensory applications, or permselective membranes.[41−46]

Altogether, the ability of molecular level control in LBL assembly allows for preparation of thin films with exceptional mechanical properties for a variety of applications and study of the molecular mechanisms of their deformation. In our research with carbon nanotubes (CNTs), we have shown preparation of free-standing films from both single-walled and multiwalled CNTs with σ_{UTS} reaching as high as 325 MPa.[5,47,48] These results are due to the ability of LBL to immobilize the high strength material inside of the polymeric matrix, allowing for more effective load transfer than in many other composites, and due to the ability of achieving high loadings without phase segregation. Clearly these results are encouraging for preparation of novel, high strength materials, and further improvements are expected. At the same time, the survey of the field also reveals two quite important issues: (1) the existing design rules[49−51] and theories are not entirely applicable to high volume fraction composites and they do not properly address the issue of interfacial interactions of components and (2) the mechanical properties of the nanocomposites are still much below those for mechanical parameters of individual nanoscale inorganic components such as nanotubes, nanowires, platelets, etc.

In an attempt at preparing an even stronger PE−MTM nanocomposite and with a goal of better understanding of the nanoscale and molecular mechanics of the composites, we have hypothesized that replacing PDDA with stronger PE will result in further improvement of the mechanical properties. We have chosen to work with a natural polymer, chitosan (CH), which not only possesses quite high strength ($\sigma_{UTS} \approx 110$ MPa, $E \approx 2$ GPa) in comparison to PDDA ($\sigma_{UTS} \approx 12$ MPa, $E \approx 0.2$ GPa) but also has excellent biocompatibility, biodegradability, nontoxicity, and antibacterial properties.[52] At the same time, the importance of CH has already been shown in several examples of LBL films for wide variety of applications: optically active films,[53−55] biodegradable thin films,[56,57] biosensors,[22,58−61] electrochemical and electrochromic materials,[62−64] drug delivery multilayered capsules,[65] and coatings for improvement of cytocompatibility.[66,67]

In this study we present our results from LBL assembly of CH with MTM. We show preparation of highly uniform free-standing films and mechanical strength evaluation of the resulting nanocomposite. Film homogeneity and deposition was monitored using UV−vis spectroscopy and scanning electron microscopy (SEM). Loading of inorganic material was characterized with thermogravimetric analysis (TGA), and the strength of free-standing films was determined with standard stress−strain curves. Contrary to our expectations and theoretical predictions, the CH−MTM composite showed significantly lower mechanical properties when compared to the PDDA−MTM system, with $\sigma_{UTS} = 81 \pm 12$ MPa and $E = 6.1 \pm 0.8$ GPa. Equally surprisingly, the composite showed lower σ_{UTS} than the pure polymer itself. Comparison of "plane-to-plane" adhesion revealed a factor of ~4 stronger adhesion in PDDA-MTM films than in CH−MTM. In the case of the PDDA−MTM system, the excellent mechanical properties were associated along with other parameters with coiled conformation of the flexible PDDA chains, which is related to the presence of sacrificial bonds in natural nacre. Apparently the flexibility of the macromolecules is also critical for efficient stress dissipation and load transfer. For the CH−MTM system, lower σ_{UTS} is attributed to high rigidity of the CH backbone which was observed in highly elongated conformation of the polymer chains by atomic force microscopy (AFM). Therefore, this study creates a criterion for future design of ultrastrong thin film composites, which may also be applicable to conventional blends.

CH−MTM films were prepared following similar conditions to those of the PDDA−MTM system reported previously,[38] namely, 5 min immersion of a glass slide in CH solution, 2×1 min rinse in deionized water, 1 min of air drying, and 5 min of immersion in a clay dispersion followed again by rinsing and drying steps (see Supporting Information). These conditions proved to be sufficient for successful assembly giving a very uniform and homogeneous multilayer structure. AFM characterization of a single bilayer (CH + MTM layers) revealed high density of MTM platelets adsorbed parallel to the substrate on a CH surface just as in the PDDA−MTM composite presented before (Figure 1). The AFM images also show that some of the adsorbing MTM platelets are composed of several-sheet-thick stacks resulting from incomplete exfoliation of clay. Overall the surface coverage is dense and relatively uniform for a single bilayer.

Having observed chemical compatibility of CH and MTM, LBL structures were prepared on microscope glass slides and polished silicon wafers in order to characterize assembly using UV−vis spectroscopy and ellipsometry. In typical PE-MTM assemblies, increasing number of deposited bilayers

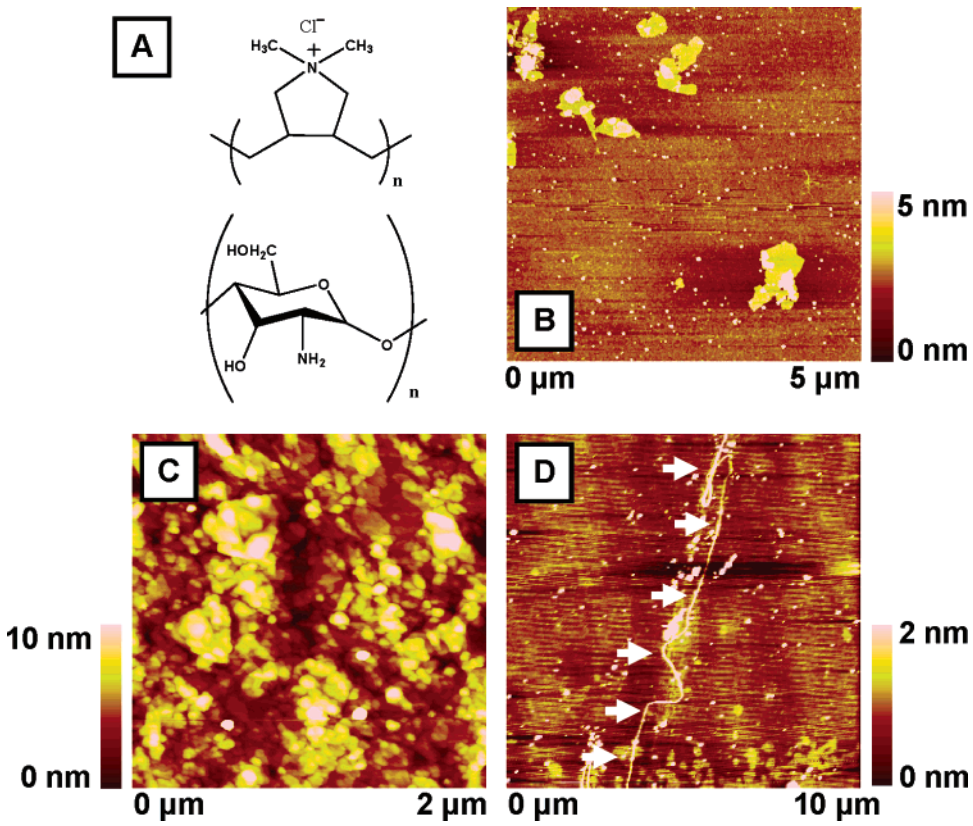

Figure 1. (A) Structure of PDDA (top) and CH (bottom) polymers. (B) AFM of a dilute solution of MTM adsorbed on a single layer of CH. (C) AFM of a single bilayer of CH + MTM adsorbed on a silicon wafer surface (height). (D) AFM image of a single chain of CH adsorbed on a silicon wafer surface.

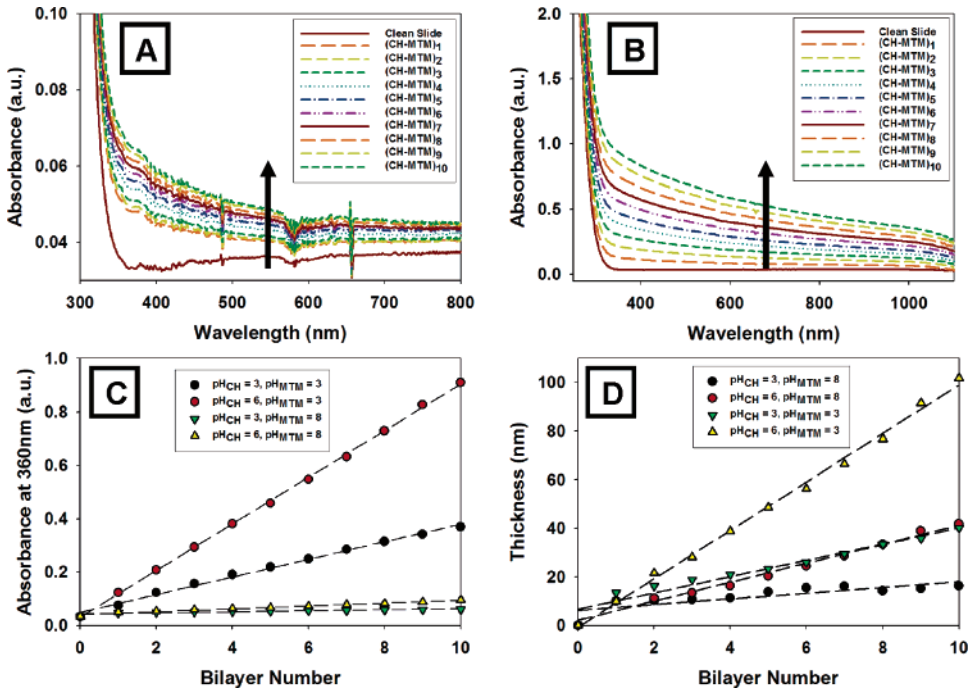

Figure 2. (A) Compilation of UV−vis absorbance spectra for CH−MTM assembly for the first 10 bilayers with pH = 3 and pH = 8 of the two components, respectively. (B) Compilation of UV−vis spectra for pH = 6 and pH = 3 of CH and MTM, respectively. (C) Linear regressions of absorbance vs bilayer number for CH−MTM assembled with indicated pH conditions. (D) Ellipsometry results for CH−MTM assembly under indicated pH conditions.

results in a linear increase of optical density. The same was observed for the CH−MTM composite (parts A and B of Figure 2). We have also observed that varying the pH of MTM or CH solutions can result in substantial changes in thickness of the films (parts B and D of Figure 2). The most substantial increase in thickness was observed for low pH

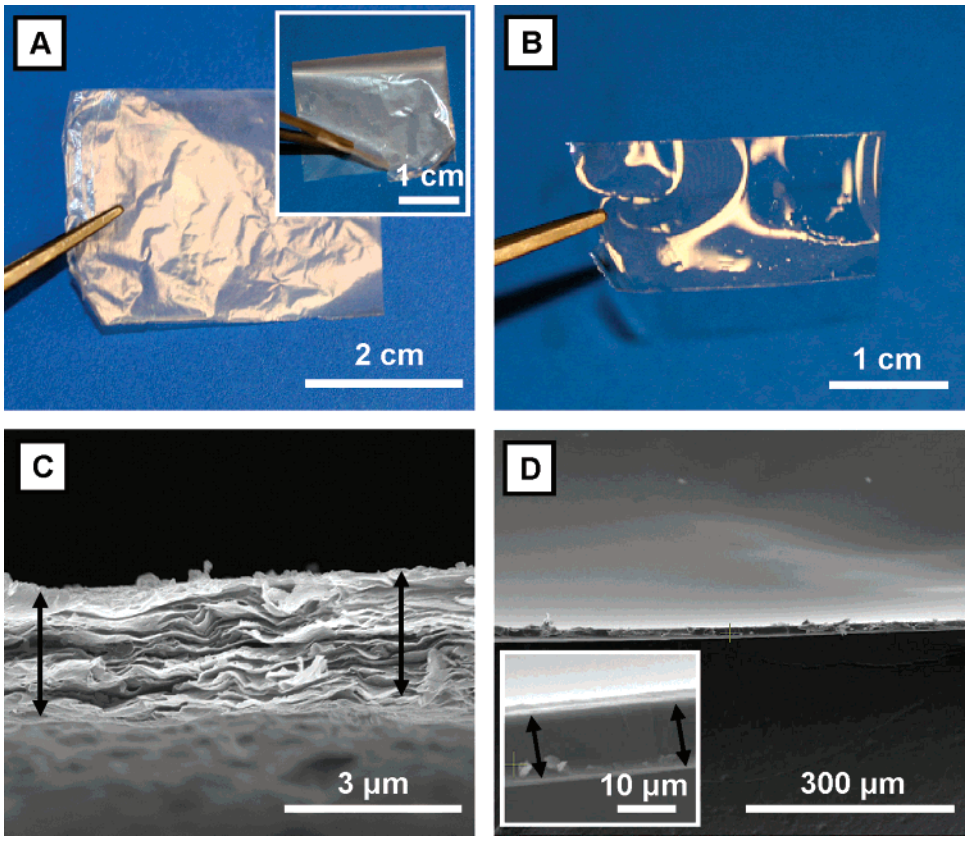

Figure 3. (A) Free-standing, 300-bilayer CH−MTM nanocomposite film. Inset shows folded film revealing good flexibility. (B) Free-standing film of CH polymer prepared by evaporation. C) SEM image of CH−MTM composite's cross section. (D) SEM image of CH polymer film's cross section. Inset represents a closeup of the cross section.

of MTM and/or high pH of CH solutions. This is likely to be a result of two factors: (1) decreasing the pH of MTM results in aggregation of the platelets which increases thickness of the MTM layer and (2) the primary amino groups on CH, with pK_a value of ~6.4, are sensitive to the pH of the environment, which has an effect on both adsorption of MTM and conformation of the polymer chains.[68] When using low pH of MTM solution, the pH of the CH layer on the glass slide is kept below its pK_a value which helps in adsorption of the aggregated platelets. Increasing pH of CH deprotonates the amino groups allowing for more flexible conformation of the chains as was shown for CH adsorbing on mica and much thicker polymer layers.[68]

Overall, in all of the cases, when absorbance was plotted as a function of a bilayer number for a particular wavelength, a linear growth was observed (Figure 2C). Similar results were also observed from ellipsometry (Figure 2D). In particular, ellipsometry showed rather slow and irregular increase in thickness for low pH CH and high pH MTM. After 10 bilayers, the thickness of the film reached only ~15 nm, giving ~3 nm per bilayer on average. For high pH of CH and low pH of MTM, the thickness of the composite increases linearly at ~10 nm per bilayer.

For proper comparison with PDDA−MTM, CH−MTM films were prepared using the same conditions as used for the former composite: pH = 3 for CH and pH = 8 for MTM (as dissolved). Several samples of 300-bilayer films were prepared on microscope glass slides, dried at 60 °C for 1 h,

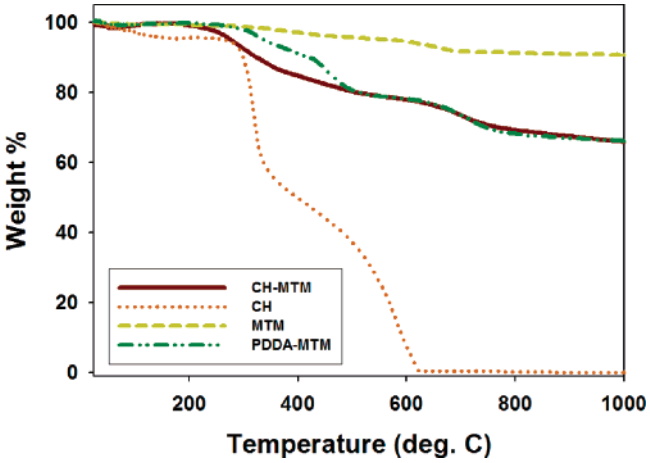

Figure 4. TGA comparison of different PE−MTM composites.

and then detached from the surface using an HF method described in the experimental section. The films were highly uniform and flexible. Interestingly, they were much more transparent when compared to 300-bilayer PDDA−MTM films (Figure 3A). We believe that this effect is a result of a good dispersion of the nanoscopic filler, the nanoscale dimensions of the filler, as well as decreased surface roughness of the CH−MTM films as compared to PDDA−MTM which decreases light scattering.

SEM characterization of the free-standing films revealed uniform thickness of 2.2 ± 0.2 μm giving an average

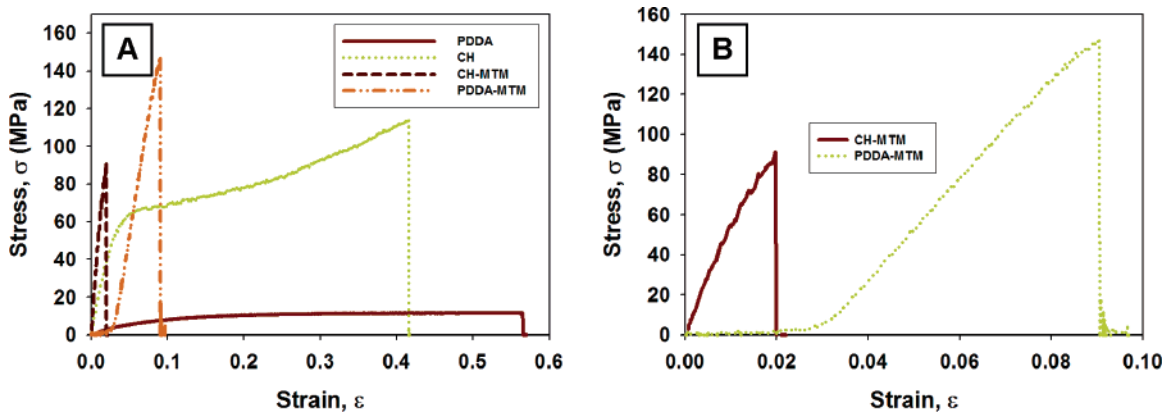

Figure 5. (A) Stress−strain curves for CH, PDDA, PDDA−MTM, and CH−MTM. (B) Comparison of CH−MTM and PDDA−MTM stress−strain curves.

Table 1. Comparison of the Mechanical Properties for Composites and Pure Polymers

	Ultimate Strength, σ_{UTS} (MPa)	Young's Modulus, E (GPa)	Fracture Strain, ϵ (%)	Toughness (MJ/m^3)
PDDA	12 ± 4	0.16 ± 0.03	48 ± 9	4.7 ± 2.0
CH	108 ± 15	1.9 ± 0.3	42 ± 9	31.6 ± 8.8
PDDA−MTM	100 ± 10	11 ± 2	8.4 ± 0.7	∼0.5
CH−MTM	81 ± 12	6.1 ± 0.8	1.9 ± 0.6	0.9 ± 0.4

thickness per bilayer of ∼7 nm. This thickness is higher than that reported from ellipsometry, and we attribute it to the initial lag of deposition which is often present in LBL assemblies as well as increased surface roughness of the final film. The cross section also revealed similar, well-defined stratified structure which was observed previously in the PDDA−MTM composite (Figure 2C). Given that there are no available mechanical properties, data for the PDDA and high molecular weight CH, we have also cast films of the two by evaporation of the solutions used for composites preparation (parts B and D of Figure 2, also see Supporting Information). Both of the films, due to their hygroscopic nature, were kept well dried until testing. TGA analysis revealed exceptionally high loading of the inorganic material at ∼80 wt % (∼42 vol %) (Figure 4). Nearly identical loading was found for the PDDA−MTM composite, although PDDA showed better thermal stability in comparison to CH.

Having obtained the thickness from SEM analysis, the material was cut into thin strips and subjected to a standard stretching test in order to obtain stress (σ) vs strain (ϵ) plots. Figure 5 shows typical stress−strain responses of PDDA, CH, PDDA−MTM, and CH−MTM, and Table 1 summarizes all of the mechanical properties. In the case of PDDA there is an order of magnitude increase in σ_{UTS} and nearly 2 orders of magnitude in E. At the same time, the toughness of the composite (estimated from the area under the curve) has decreased by an order of magnitude. In the case of CH the increase in E is not as large, only a factor of ∼3 and σ_{UTS} has actually decreased by ∼25%. This is a surprising result since we have anticipated substantial increase in the stiffness and especially the ultimate strength. For comparison, literature values for mechanical properties of CH report similar or higher results for the modulus and slightly lower results for the strength, ∼40−100 MPa.[69] While direct comparison cannot be made between our polymer and those reported in the literature in order to confirm our results (differences in sample preparation technique, solvent, and molecular weight), the increase over the literature reported

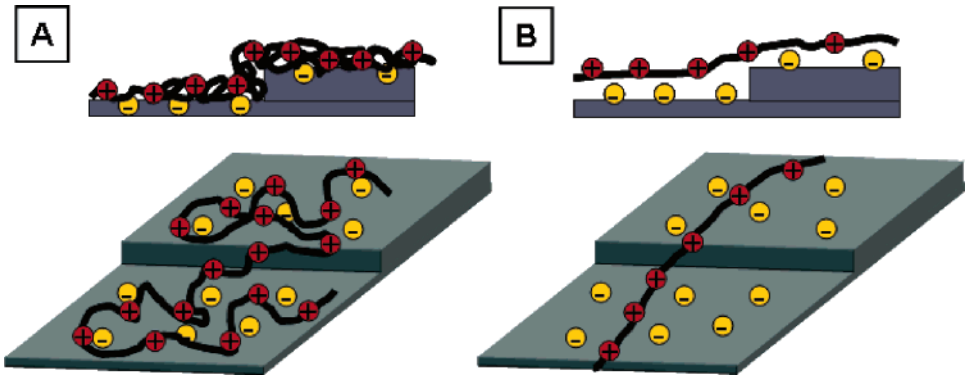

Figure 6. Graphical representation of polyelectrolyte folding and presumed structure of adsorbing chains for (A) PDDA−MTM and (B) CH−MTM nanocomposites. Top images represent a side view of an edge of a clay nanosheets adsorbed on a substrate.

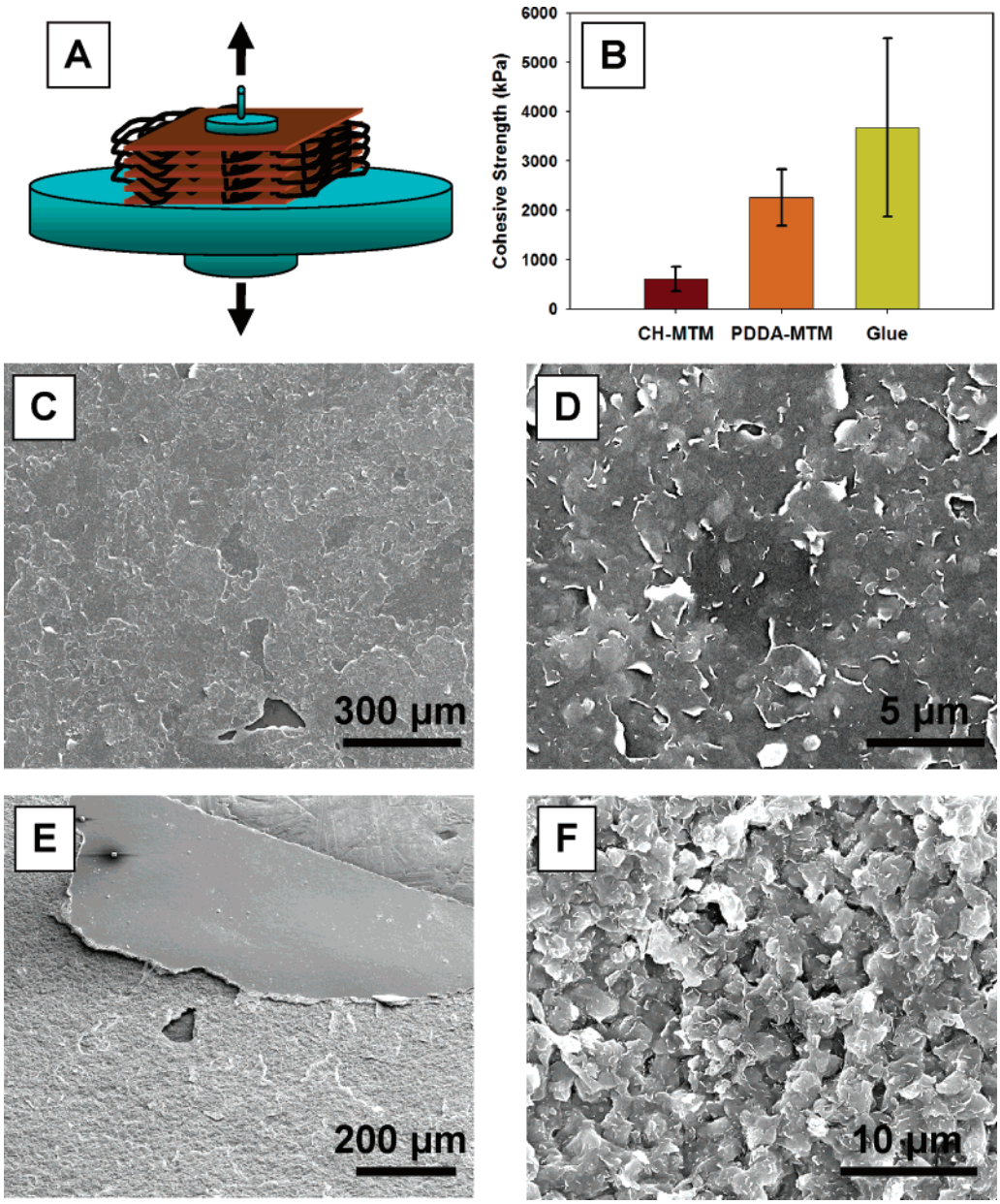

Figure 7. Cohesive strength results: (A) graphical representation of experimental setup; (B) comparison of the results; (C and D) CH−MTM film after planes separation; (E and F) PDDA−MTM film after planes separation.

values is still very small in comparison to PDDA−MTM composite. Furthermore, theoretical predictions using the well-known Halpin−Tsai's composite theory[51] or the somewhat similar continuum model of Jager−Fratzl[49] for "nacre-like" biocomposites give $E \sim 101$ GPa and $E \sim 110$ GPa, respectively, when applied to the CH−MTM system (see Supporting Information for calculations). Clearly the calculated values are more than an order of magnitude higher than those achieved.

The weakening of the material when a stronger nanoscale component is incorporated may remind one of the case with classical polymer/clay nanocomposites. Inclusion of a small amount of inorganic filler (usually at ≤5 wt %) results in increase of ultimate stress, Young's modulus, and fracture strain,[70−72] while above this threshold mechanical properties decrease in most cases. This effect is attributed to the decreased dispersability of clay sheets at high loadings and formation of large scale nonuniformities. In the case of LBL films the effect is likely to have a different nature because the spatial distribution of the components remains uniform.

Mechanical strength of clay nanocomposites is a cumulative product of many factors, e.g., degree of clay exfoliation, homogeneity of the dispersion, or strength of polymer−clay interfacial adhesion. As can be seen from the data provided above, the loading of the clay, the degree of exfoliation, the overall homogeneity, and orientation of clay platelets in CH−MTM and PDDA−MTM are quite close to each other (see Figures 1−4). To understand the reasons behind these low mechanical properties, we have investigated adsorption of CH chains with AFM. Topographic AFM images revealed highly elongated chains adsorbed on the surface (Figure 1D) and can be contrasted with our results for PDDA, where we have shown that more than 85% of chains adsorb in highly coiled conformation.[38] This can be attributed to the well-

known high rigidity of CH due to its polysaccharide backbone. For PDDA−MTM we have shown that this coiled conformation is directly related to the unusual toughening mechanism of nacre or spider silk[73] due to sacrificial bonds between the different parts of the polymeric chain. One can also suggest that flexibility of the polymer directly affects the stress dissipation and load transfer from the organic matrix to the inorganic nanoscale component, i.e., MTM sheets in this case. We believe that high rigidity results in poor CH−MTM interaction, thus contributing to lowering of the mechanical properties, which is not considered in the theoretical models. The CH chain cannot find an optimal conformation on the surface of the MTM, which would result in maximum attraction due to lack of flexibility, which is possible for PDDA (Figure 6). The attraction energies to consider here include electrostatic attraction, hydrogen bonding, and van der Waals forces. All this creates a complex, topographically uneven, and quite stochastic force field map, which is difficult to adjust to and acquire a reasonable degree of adhesion unless different parts of the backbone can move fairly independently of each other, which cannot be realized in the rigid CH molecule.

To test this hypothesis we have compared the cohesive strength between CH−MTM and PDDA-MTM composites (see Supporting Information). If the hypothesis is correct, it must inevitably result in the lower adhesion of one multilayer to another. Indeed, the force required to break the contact between disks (Figure 7) showed that the strength of adhesion in PDDA−MTM composite is a factor of ∼4 higher than that in the CH−MTM, 2260 ± 570 kPa vs 670 ± 250 kPa, which directly proves the fact that CH does not provide as strong adhesion between the multilayers and importance of conformational freedom during adsorption. Because of the low energy of attraction between CH and MTM, the strength of individual molecules cannot come into play when films undergo in-plane deformation.

In conclusion, LBL technique is a tool which enables manufacturing of the composite via bottom-up fabrication method, a few nanometers at a time, which in turn allows for incorporation of high amounts of the inorganic filler with homogeneous distribution throughout the composite. Also important is parallel orientation of all the platelets, which greatly helps in understanding the processes and achieving desirable mechanical characteristics. Against expectations and theoretical predictions, the mechanical properties of a new nanocomposite incorporating one of the strongest natural polymers, CH, were found to be noticeably lower than for a structurally similar composite with drastically weaker polymer, i.e., PDDA. The decrease in mechanical properties was attributed to high rigidity of the polymer resulting in the poor interfacial adhesion with the clay. This study (1) shows unorthodox nature of the behavior of nanocomposites, (2) opens the door to the detailed understanding of the mechanics at nanoscale, and (3) provides a critical criterion for the selection of the organic matrix for advanced nanocomposites necessary for a wide variety of applications from energy conversion to biotechnology.

Acknowledgment. P. Podsiadlo thanks the Fannie and John Hertz Foundation for support of his work through a graduate fellowship. Authors acknowledge the staff of the Electron Microscopy Analysis Laboratory and their sponsor, NSF through grant #DMR-0320740. N.A.K. thanks AFOSR, NAVY, and NSF for the support of this project. The authors thank Dr. Vladimir A. Sinani for assistance during this project.

Supporting Information Available: A description of experimental details including materials, layer-by-layer assembly of CH−MTM films, and instrumental analysis, figures showing a SEM of pure PDDA film cross section, experimental setup for plane-to-plane adhesion measurements, and plates after plane-to-plane adhesion test, and details of the Halpin−Tsai and Jaeger−Fratzl model calculations of CH-MTM nanocomposite modulus. This material is available free of charge via the Internet at http://pubs.acs.org.

References

(1) Decher, G. *Science* **1997**, *277*, 1232.
(2) Hammond, P. T. *Adv. Mater.* **2004**, *16*, 1271.
(3) Ingersoll, D.; Kulesza, P. J.; Faulkner, L. R. *J. Electrochem. Soc.* **1994**, *141*, 140.
(4) Kotov, N. A.; Dekany, I.; Fendler, J. H. *J. Phys. Chem.* **1995**, *99*, 13065.
(5) Mamedov, A. A.; Kotov, N. A.; Prato, M.; Guldi, D. M.; Wicksted, J. P.; Hirsch, A. *Nat. Mater.* **2002**, *1*, 190.
(6) Jiang, C.; Ko, H.; Tsukruk, V. V. *Adv. Mater.* **2005**, *17*, 2127.
(7) Keller, S. W.; Kim, H. N.; Mallouk, T. E. *J. Am. Chem. Soc.* **1994**, *116*, 8817.
(8) Cooper, T. M.; Campbell, A. L.; Crane, R. L. *Langmuir* **1995**, *11*, 2713.
(9) He, J. A.; Valluzzi, R.; Yang, K.; Dolukhanyan, T.; Sung, C.; Kumar, J.; Tripathy, S. K.; Samuelson, L.; Balogh, L.; Tomalia, D. A. *Chem. Mater.* **1999**, *11*, 3268.
(10) Araki, K.; Wagner, M. J.; Wrighton, M. S. *Langmuir* **1996**, *12*, 5393.
(11) Lvov, Y.; Onda, M.; Ariga, K.; Kunitake, T. *J. Biomater. Sci., Polym. Ed.* **1998**, *9*, 345.
(12) Richert, L.; Lavalle, P.; Vautier, D.; Senger, B.; Stoltz, J. F.; Schaaf, P.; Voegel, J. C.; Picart, C. *Biomacromolecules* **2002**, *3*, 1170.
(13) Boulmedais, F.; Ball, V.; Schwinte, P.; Frisch, B.; Schaaf, P.; Voegel, J. C. *Langmuir* **2003**, *19*, 440.
(14) Lvov, Y.; Decher, G.; Sukhorukov, G. *Macromolecules* **1993**, *26*, 5396.
(15) Hong, J. D.; Lowack, K.; Schmitt, J.; Decher, G. *Prog. Colloid Polym. Sci.* **1993**, *93*, 98.
(16) Lvov, Y.; Ariga, K.; Kunitake, T. *Chem. Lett.* **1994**, (12), 2323.
(17) Yoo, P. J.; Nam, K. T.; Qi, J.; Lee, S. K.; Park, J.; Belcher, A. M.; Hammond, P. T. *Nat. Mater.* **2006**, *5*, 234.
(18) Tang, Z.; Wang, Y.; Podsiadlo, P.; Kotov, N. A. *Adv. Mater.* **2006**, *18*, 3203.
(19) Zhai, L.; Cebeci, F. C.; Cohen, R. E.; Rubner, M. F. *Nano Lett.* **2004**, *4*, 1349.
(20) Zhai, L.; Berg, M. C.; Cebeci, F. C.; Kim, Y.; Milwid, J. M.; Rubner, M. F.; Cohen, R. E. *Nano Lett.* **2006**, *6*, 1213.
(21) Ellis, D. L.; Zakin, M. R.; Bernstein, L. S.; Rubner, M. F. *Anal. Chem.* **1996**, *68*, 817.
(22) Constantine, C. A.; Mello, S. V; Dupont, A.; Cao, X.; Santos, D., Jr.; Oliveira, O. N., Jr.; Strixino, F. T.; Pereira, E. C.; Cheng, T.; Defrank, J. J.; Leblanc, R. M. *J. Am. Chem. Soc.* **2003**, *125*, 1805.
(23) Koktysh, D. S.; Liang, X.; Yun, B. G.; Pastoriza-Santos, I.; Matts, R. L.; Giersig, M.; Serra-Rodriguez, C.; Liz-Marzan, L. M.; Kotov, N. A. *Adv. Funct. Mater.* **2002**, *12*, 255. 2002.
(24) Wood, K. C.; Chuang, H. F.; Batten, R. D.; Lynn, D. M.; Hammond, P. T. *Proc. Natl. Acad. Sci. U.S.A.* **2006**, *103*, 10207.
(25) Jewell, C. M.; Zhang, J.; Fredin, N. J.; Lynn, D. M. *J. Controlled Release* **2005**, *106*, 214.
(26) Hiller, J.; Mendelsohn, J. D.; Rubner, M. F. *Nat. Mater.* **2002**, *1*, 59.

(27) DeLongchamp, D. M.; Hammond, P. T. *Adv. Funct. Mater.* **2004**, *14*, 224.
(28) Moriguchi, I.; Fendler, J. H. *Chem. Mater.* **1998**, *10*, 2205.
(29) Heuberger, R.; Sukhorukov, G.; Voeroes, J.; Textor, M.; Moehwald, H. *Adv. Funct. Mater.* **2005**, *15*, 357.
(30) Tokuhisa, H.; Hammond, P. T. *Adv. Funct. Mater.* **2003**, *13*, 831.
(31) Zhang, J.; Senger, B.; Vautier, D.; Picart, C.; Schaaf, P.; Voegel, J. C.; Lavalle, P. *Biomaterials* **2005**, *26*, 3353.
(32) Mamedov, A. A.; Belov, A.; Giersig, M.; Mamedova, N. N.; Kotov, N. A. *J. Am. Chem. Soc.* **2001**, *123*, 7738.
(33) Wang, D.; Rogach, A. L.; Caruso, F. *Nano Lett.* **2002**, *2*, 857.
(34) Liu, J.; Cheng, L.; Song, Y.; Liu, B.; Dong, S. *Langmuir* **2001**, *17*, 6747.
(35) Shen, Y.; Liu, J.; Jiang, J.; Liu, B.; Dong, S. *J. Phys. Chem. B* **2003**, *107*, 9744.
(36) Nolte, A. J.; Rubner, M. F.; Cohen, R. E. *Langmuir* **2004**, *20*, 3304.
(37) Mamedov, A. A.; Kotov, N. A. *Langmuir* **2000**, *16*, 5530.
(38) Tang, Z.; Kotov, N. A.; Magonov, S.; Ozturk, B. *Nat. Mater.* **2003**, *2*, 413.
(39) Malikova, N.; Pastoriza-Santos, I.; Schierhorn, M.; Kotov, N. A.; Liz-Marzan, L. M. *Langmuir* **2002**, *18*, 3694.
(40) Podsiadlo, P.; Paternel, S.; Rouillard, J. M.; Zhang, Z.; Lee, J.; Lee, J. W.; Gulari, E.; Kotov, N. A. *Langmuir* **2005**, *21*, 11915.
(41) Lvov, Y.; Ariga, K.; Ichinose, I.; Kunitake, T. *J. Am. Chem. Soc.* **1995**, *117*, 6117.
(42) Ku, B. C.; Froio, D.; Steeves, D.; Kim, D. W.; Ahn, H.; Ratto, J. A.; Blumstein, A.; Kumar, J.; Samuelson, L. A. *J. Macromol. Sci. Pure* **2004**, *A41*, 1401.
(43) Kim, D. W.; Choi, H. S.; Lee, C.; Blumstein, A.; Kang, Y. *Electrochim. Acta* **2004**, *50*, 659.
(44) Guo, Z.; Shen, Y.; Zhao, F.; Wang, M.; Dong, S. *Analyst* **2004**, *129*, 657.
(45) Yamamoto, T.; Umemura, Y.; Sato, O.; Einaga, Y. *Chem. Lett.* **2004**, *33*, 500.
(46) Li, Z.; Hu, N. *J. Electroanal. Chem.* **2003**, *558*, 155.
(47) Qin, S.; Qin, D.; Ford, W. T.; Zhang, Y.; Kotov, N. A. *Chem. Mater.* **2005**, *17*, 2131.
(48) Olek, M.; Ostrander, J.; Jurga, S.; Moehwald, H.; Kotov, N.; Kempa, K.; Giersig, M. *Nano Lett.* **2004**, *4*, 1889.
(49) Gao, H.; Ji, B.; Jager, I. L.; Arzt, E.; Fratzl, P. *Proc. Natl. Acad. Sci. U.S.A.* **2003**, *100*, 5597.
(50) Jager, I.; Fratzl, P. *Biophys. J.* **2000**, *79*, 1737.
(51) Halpin, J. C.; Kardos, J. L. *Polym. Eng. Sci.* **1976**, *16*, 344.
(52) Kumar, M. N. V. R. *React. Funct. Polym.* **2000**, *46*, 1.
(53) Camilo, C. S.; dos Santos, D. S., Jr.; Rodrigues, J. J., Jr.; Vega, M. L.; Campana Filho, S. P.; Oliveira, O. N., Jr.; Mendonca, C. R. *Biomacromolecules* **2003**, *4*, 1583.
(54) dos Santos, D. S., Jr.; Bassi, A.; Rodrigues, J. J., Jr.; Misoguti, L.; Oliveira, O. N., Jr.; Mendonca, C. R. *Biomacromolecules* **2003**, *4*, 1502.
(55) Sotero Dos Santos, D., Jr.; Bassi, A.; Misoguti, L.; Ginani, M. F.; Novais De Oliveira, O., Jr.; Mendonca, C. R. *Macromol. Rapid Commun.* **2002**, *23*, 975.
(56) Serizawa, T.; Yamaguchi, M.; Akashi, M. *Macromolecules* **2002**, *35*, 8656.
(57) Tachaboonyakiat, W.; Serizawa, T.; Endo, T.; Akashi, M. *Polym. J.* **2000**, *32*, 481.
(58) Constantine, C. A.; Gattas-Asfura, K. M.; Mello, S. V.; Crespo, G.; Rastogi, V.; Cheng, T. C.; Defrank, J. J.; Leblanc, R. M. *Langmuir* **2003**, *19*, 9863.
(59) Xu, X. H.; Han, B.; Fu, Y. S.; Han, J.; Shi, H. B.; Wu, B.; Han, S.; Chen, Q. *J. Mater. Sci. Lett.* **2003**, *22*, 695.
(60) dos Santos, D. S., Jr.; Riul, A., Jr.; Malmegrim, R. R.; Fonseca, F. J.; Oliveira, O. N., Jr.; Mattoso, L. H. C. *Macromol. Biosci.* **2003**, *3*, 591.
(61) Riul, A.; de Sousa, H. C.; Malmegrim, R. R.; dos Santos, D. S.; Carvalho, A. C. P. L.; Fonseca, F. J.; Oliveira, O. N.; Mattoso, L. H. C. *Sens. Actuators, B* **2004**, *B98*, 77.
(62) Huguenin, F.; dos Santos, D. S., Jr.; Bassi, A.; Nart, F. C.; Oliveira, O. N., Jr. *Adv. Funct. Mater.* **2004**, *14*, 985.
(63) Huguenin, F.; Nart, F. C.; Gonzalez, E. R.; Oliveira, O. N., Jr. *J. Phys. Chem. B* **2004**, *108*, 18919.
(64) Huguenin, F.; Gonzalez, E. R.; Oliveira, O. N., Jr. *J. Phys. Chem. B* **2005**, *109*, 12837.
(65) Ye, S.; Wang, C.; Liu, X.; Tong, Z. *J. Controlled Release* **2005**, *106*, 319.
(66) Zhu, Y.; Gao, C.; He, T.; Liu, X.; Shen, J. *Biomacromolecules* **2003**, *4*, 446.
(67) Liu, Y.; He, T.; Gao, C. *Colloids Surf., B* **2005**, *46*, 117.
(68) Claesson, P. M.; Ninham, B. W. *Langmuir* **1992**, *8*, 1406.
(69) Lazaridou, A.; Biliaderis, C. G. *Carbohydr. Polym.* **2002**, *48*, 179.
(70) Srivastava, S. K.; Pramanik, M.; Acharya, H. *J. Polym. Sci., Part B*: *Polym. Phys.* **2006**, *44*, 471.
(71) Jordan, J.; Jacob, K. I.; Tannenbaum, R.; Sharaf, M. A.; Jasiuk, I. *Mater. Sci. Eng., A* **2005**, *A393*, 1.
(72) Ray, S. S.; Bousmina, M. *Prog. Mater. Sci.* **2005**, *50*, 962.
(73) Smith, B. L.; Schaffer, T. E.; Viani, M.; Thompson, J. B.; Frederick, N. A.; Kind, J.; Belcher, A.; Stucky, G. D.; Mors, D. E.; Hansma, P. K. *Nature* **1999**, *399*, 761.

NL0700649